Encapsulation of Conjugated Polymers in Block Copolymer−Templated Mesostructured Oxides: A Cosolvent Assisted Approach

ARTICLE *in* CHEMISTRY OF MATERIALS · OCTOBER 2009

Impact Factor: 8.35 · DOI: 10.1021/cm900708z

5 AUTHORS, INCLUDING:

Saar Kirmayer
Weizmann Institute of Science
18 PUBLICATIONS **919** CITATIONS

SEE PROFILE

CHEMISTRY OF MATERIALS
Article

Chem. Mater. **2009,** *21,* 4387–4396 4387
DOI:10.1021/cm900708z

Encapsulation of Conjugated Polymers in Block Copolymer-Templated Mesostructured Oxides: A Cosolvent Assisted Approach

Saar Kirmayer, Shany Neyshtadt, Avigail Keller, Dina Okopnik, and Gitti L. Frey*

Department of Materials Engineering, Technion − Israel Institute of Technology, Haifa 32000, Israel

Received March 12, 2009. Revised Manuscript Received July 30, 2009

The deposition of conjugated polymer-incorporated mesostructured metal oxide films, with control over charge and energy transfer, is reported. The conjugated polymer guests in xylene are dropwise added into the polar precursor solution including metal oxide precursor species and block copolymer structure directing agent. The hydrophobicity and relatively low volatility of the xylene cosolvent, previously used for pore swelling, drives the conjugated polymers into the hydrophobic domains of the self-organizing block copolymer mesophases that template the metal oxide scaffold. This method has permitted the deposition of conjugated polymer-incorporated 2D-hexagonal and 3D-cubic silica and titania films from predominantly aqueous conditions, evident from small-angle X-ray scattering and transmission electron microscopy. Spatially locating the conjugated polymer guests in the organic domains of the inorganic−organic mesostructure suppresses energy transfer between polymer chains in adjacent micelles. Hence, incorporation of red- and blue-emitting polymers in separate micelles results in simultaneous red and blue emission, that is, white light generation. The efficacy of the conjugated polymer-incorporated metal oxide films for optoelectronic devices is demonstrated by integrating the white-emitting 3D-cubic silica film, which supports carrier transport along the continuous through-film conjugated polymer pathways, as the active layer in white light emitting devices.

Introduction

Periodic mesoporous materials have motivated extensive research since their discovery in the early 90s[1] toward their utilization in a variety of applications including catalysis supports,[2] separation technology,[3] sensors,[4,5] and optoelectronic devices.[6−8] Metal-oxide mesoporous solids are conventionally synthesized using sol−gel chemistry in the presence of surface directing agents (surfactants), which self-organize into mesophases templating the concurrently polymerizing inorganic matrix.[9−12] The surfactants are then removed by calcination leaving a mesoporous material with a unique combination of high surface area and long-range spatial order. The spatial order of the templated metal−solid, that is, the type and lattice parameters of the obtained mesophase, are determined by the surfactant type,[13,14] the composition of the precursor sol solution,[15] and the reaction temperature.[16] However, it has been shown that the pores could be expanded by adding organic cosolvents to the ethanolic/aqueous precursor sol solution. The cosolvents, such as 1,3,5-trimethylbenzene,[17] triisopropylbenzene,[18] polypropylene glycol,[19] amines,[20] or alkanes,[21] are less volatile compared to ethanol and water and compatible with

*Corresponding author. E-mail: gitti@tx.technion.ac.il.

(1) Kresge, C. T.; Leonowicz, M. E.; Roth, W. J.; Vartuli, J. C.; Beck, J. S. *Nature* **1992**, *359*(6397), 710–712.
(2) Feng, Y. F.; Yang, X. Y.; Di, Y.; Du, Y. C.; Zhang, Y. L.; Xiao, F. S. *J. Phys. Chem. B* **2006**, *110*(29), 14142–14147.
(3) Athens, G. L.; Ein-Eli, Y.; Chmelka, B. F. *Adv. Mater.* **2007**, *19*(18), 2580–2587.
(4) Miled, O. B.; Grosso, D.; Sanchez, C.; Livage, J. *J. Phys. Chem. Solids* **2004**, *65*(10), 1751–1755.
(5) Tao, S. Y.; Li, G. T.; Zhu, H. S. *J. Mater. Chem.* **2006**, *16*(46), 4521–4528.
(6) Coakley, K. M.; Liu, Y. X.; McGehee, M. D.; Frindell, K. L.; Stucky, G. D. *Adv. Funct. Mater.* **2003**, *13*(4), 301–306.
(7) Bach, U.; Lupo, D.; Comte, P.; Moser, J. E.; Weissortel, F.; Salbeck, J.; Spreitzer, H.; Gratzel, M. *Nature* **1998**, *395*(6702), 583–585.
(8) Zukalova, M.; Zukal, A.; Kavan, L.; Nazeeruddin, M. K.; Liska, P.; Gratzel, M. *Nano Lett.* **2005**, *5*(9), 1789–1792.
(9) Brinker, C. J.; Lu, Y. F.; Sellinger, A.; Fan, H. Y. *Adv. Mater.* **1999**, *11*(7), 579–585.
(10) Monnier, A.; Schuth, F.; Huo, Q.; Kumar, D.; Margolese, D.; Maxwell, R. S.; Stucky, G. D.; Krishnamurty, M.; Petroff, P.; Firouzi, A.; Janicke, M.; Chmelka, B. F. *Science* **1993**, *261*(5126), 1299–1303.
(11) Firouzi, A.; Kumar, D.; Bull, L. M.; Besier, T.; Sieger, P.; Huo, Q.; Walker, S. A.; Zasadzinski, J. A.; Glinka, C.; Nicol, J.; Margolese, D.; Stucky, G. D.; Chmelka, B. F. *Science* **1995**, *267*(5201), 1138–1143.
(12) Zhao, D.; Yang, P.; Melosh, N.; Feng, J.; Chmelka, B. F.; Stucky, G. D. *Adv. Mater.* **1998**, *10*(16), 1380–1385.
(13) Crepaldi, E. L.; Soler-Illia, G. J. d. A.; Grosso, D.; Cagnol, F.; Ribot, F.; Sanchez, C. *J. Am. Chem. Soc.* **2003**, *125*(32), 9770–9786.
(14) Dovgolevsky, E.; Kirmayer, S.; Lakin, E.; Yang, Y.; Brinker, C. J.; Frey, G. L. *J. Mater. Chem.* **2008**, *18*(4), 423–436.
(15) Alberius, P. C. A.; Frindell, K. L.; Hayward, R. C.; Kramer, E. J.; Stucky, G. D.; Chmelka, B. F. *Chem. Mater.* **2002**, *14*(8), 3284–3294.
(16) Khushalani, D.; Kuperman, A.; Ozin, G. A.; Tanaka, K.; Garces, J.; Olken, M. M.; Coombs, N. *Adv. Mater.* **1995**, *7*(10), 842–846.
(17) Yang, P. D.; Zhao, D. Y.; Margolese, D. I.; Chmelka, B. F.; Stucky, G. D. *Nature* **1998**, *396*(6707), 152–155.
(18) Luechinger, M.; Pirngruber, G. D.; Lindlar, B.; Laggner, P.; Prins, R. *Microporous Mesoporous Mater.* **2005**, *79*(1−3), 41–52.
(19) Park, B.-G.; Guo, W.; Cui, X.; Park, J.; Ha, C.-S. *Microporous Mesoporous Mater.* **2003**, *66*(2−3), 229–238.
(20) Sayari, A.; Kruk, M.; Jaroniec, M.; Moudrakovski, I. L. *Adv. Mater.* **1998**, *10*(16), 1376–1379.
(21) Zhang, H.; Sun, J.; Ma, D.; Weinberg, G.; Su, D. S.; Bao, X. *J. Phys. Chem. B* **2006**, *110*(51), 25908–25915.

Published on Web 09/15/2009

the aqueous/ethanolic precursor sol solution. Ethanol evaporation during film processing induces surfactant micellization and incorporation of the cosolvent molecules into the hydrophobic cores of the micelles. The cosolvent molecules are then removed with the surfactant in the calcinations process, leaving a mesoporous metal-oxide framework with a pore size larger than that obtained under the same synthetic conditions but with no cosolvent.

The polar conditions of the precursor sol solution also limit the incorporation of water-immiscible guest molecules into the mesostructured metal-oxide framework. Two approaches have been suggested to overcome the incompatibility of nonpolar or highly hydrophobic organic guest molecules in polar sol−gel solvents: incorporation of the guest species into the preformed mesoporous hosts after removal of the surfactant species[6,22] or the co-assembly of the hydrophobic guest species, surfactant, and metal-oxide precursor from solution.[12,23−28] In the former, after surfactant removal the internal surfaces of the mesopores are functionalized to compatiblize the hydrophilic metal-oxide framework with the nonpolar or highly hydrophobic organic guest molecules. For example: grafting hydrophobic alkyl moieties on the pore interior surfaces permitted infiltration of hydrophobic macromolecules, conjugated polymers, into calcined mesoporous silica.[29,30]

In the second approach, the guest molecules are introduced into the precursor solution and incorporated into the mesostructured composite during its formation. To be co-assembled with the surfactant and metal oxide precursor, the guest species must be compatible with the aqueous/ethanolic sol−gel precursor solution so that they do not macroscopically phase-separate from the synthesis mixture. For example, dye molecules added to an aqueous silica-precursor solution in the presence of amphiphilic structure-directing agents have been shown to self-assemble into mesostructured silica/block-copolymer/dye composites with laser-like or optical limiting properties.[23,24,31,32] Water-soluble conjugated polyelectrolytes,[33,34] compatible with the polar ethanolic/water solutions, have also been used for the preparation of conjugated polymer-incorporated mesostructure metal oxides. Occasionally, a water-miscible organic cosolvent was required to increase dye solubility in the polar precursor solution.[35] However, these aqueous conditions are entirely infeasible for the incorporation of highly hydrophobic guest molecules, such as most conjugated polymers. Recently, THF-based sol solutions were suggested for the synthesis of hydrophobic guest-incorporated mesostructured metal oxide films.[36] Solution processing in THF permitted highly hydrophobic, high molecular weight, conjugated polymers to be directly co-assembled within the mesostructured inorganic−organic host matrices during their formation and integration of the hybrid material into optoelectronic devices including light-emitting diodes[14] and solar cells.[37] However, in situ generation of water molecules during metal-oxide condensation reduces polymer solubility in the synthesis solution and limits polymer uptake in the THF-processed mesostructured hybrid films.

Here, we suggest the use of organic solvents known to swell the surfactant template, to guide highly hydrophobic organic macromolecules into the surfactant assemblies that template the metal-oxide framework. Under these conditions, the highly hydrophobic guest species and the metal-oxide precursor, that would otherwise macrophase separate, could be co-assembled into a highly ordered hybrid material with the guest molecules positioned in the surfactant domains. This approach is demonstrated by dropwise addition of conjugated polymer or conjugated polymer mixtures in xylene, a water-immiscible organic solvent, into an aqueous or aqueous/ethanolic sol solution containing the surfactant and metal-oxide precursor. Consequently, the surfactant self-organizes into micelles with the xylene and conjugated guest molecules incorporated into the hydrophobic regions. Solvent evaporation induces surfactant mesophase formation stabilized by the high extent of metal-oxide cross-linking into mesostructured composites. Highly ordered conjugated polymer-incorporated 3D cubic, rhombohedral, hexagonal, or lamellar silica or titania nanocomposite films are obtained, as evident from transmission electron microscopy (TEM) and glancing incidence small-angle X-ray scattering (GISAXS). Photoluminescence and energy filtered TEM measurements confirm that the conjugated polymer guest molecules are positioned in the surfactant domains. The efficacy of this approach for electroluminescent devices is demonstrated by fabricating light-emitting diodes based on the 3D-cubic mesophase which possesses a continuous through-film conductive conjugated polymer network that supports carrier transport from the electrodes

(22) Cadby, A. J.; Tolbert, S. H. *J. Phys. Chem. B* **2005**, *109*(38), 17879–17886.
(23) Yang, P. D.; Wirnsberger, G.; Huang, H. C.; Cordero, S. R.; McGehee, M. D.; Scott, B.; Deng, T.; Whitesides, G. M.; Chmelka, B. F.; Buratto, S. K.; Stucky, G. D. *Science* **2000**, *287*(5452), 465–467.
(24) Scott, B. J.; Wirnsberger, G.; McGehee, M. D.; Chmelka, B. F.; Stucky, G. D. *Adv. Mater.* **2001**, *13*(16), 1231–1234.
(25) Andersson, N.; Alberius, P.; Ortegren, J.; Lindgren, M.; Bergstrom, L. *J. Mater. Chem.* **2005**, *15*(34), 3507–3513.
(26) Yamaguchi, A.; Amino, Y.; Shima, K.; Suzuki, S.; Yamashita, T.; Teramae, N. *J. Phys. Chem. B* **2006**, *110*(9), 3910–3916.
(27) Yao, Y. F.; Zhang, M. S.; Shi, J. X.; Gong, M. L.; Zhang, H. J.; Yang, Y. S. *Mater. Lett.* **2001**, *48*(1), 44–48.
(28) Steinbeck, C. A.; Ernst, M.; Meier, B. H.; Chmelka, B. F. *J. Phys. Chem. C* **2008**, *112*(7), 2565–2573.
(29) Nguyen, T. Q.; Wu, J. J.; Doan, V.; Schwartz, B. J.; Tolbert, S. H. *Science* **2000**, *288*(5466), 652–656.
(30) Nguyen, T. Q.; Wu, J.; Tolbert, S. H.; Schwartz, B. J. *Adv. Mater.* **2001**, *13*(8), 609–611.
(31) Wirnsberger, G.; Scott, B. J.; Chmelka, B. F.; Stucky, G. D. *Adv. Mater.* **2000**, *12*(19), 1450–1454.
(32) Yagi, K.; Shibata, S.; Yano, T.; Yasumori, A.; Yamane, M.; Dunn, B. *J. Sol-Gel Sci. Technol.* **1995**, *4*(1), 67–73.
(33) Hoven, C. V.; Garcia, A.; Bazan, G. C.; Nguyen, T. Q. *Adv. Mater.* **2008**, *20*(20), 3793–3810.
(34) Wang, F. K.; Bazan, G. C. *J. Am. Chem. Soc.* **2006**, *128*(49), 15786–15792.
(35) Huang, M. H.; Kartono, F.; Dunn, B.; Zink, J. I. *Chem. Mater.* **2002**, *14*(12), 5153–5162.
(36) Kirmayer, S.; Dovgolevsky, E.; Kalina, M.; Lakin, E.; Cadars, S.; Epping, J. D.; Fernandez-Arteaga, A.; Rodriguez-Abreu, C.; Chmelka, B. F.; Frey, G. L. *Chem. Mater.* **2008**, *20*(11), 3745–3756.
(37) Neyshtadt, S.; Kalina, M.; Frey, G. L. *Adv. Mater.* **2008**, *20*(13), 2541–2546.

through the film. This study demonstrates the ability to direct the self-organization of functional components into hierarchically ordered materials with control over both energy and charge transfer.

Experimental Section

Materials. Ethanol (Biolab, Israel), 0.01 M HCl (Carlo Erba, Italy), xylene (Gadot, Israel), tetraethoxysilane (TEOS 98% GC, Aldrich, Germany), titanium ethoxide (TEOT, Aldrich Germany), and 12 M concentrated hydrochloric acid, HCl (Carlo Erba, Italy) in deionixed water, were used as received. The structure-directing surfactant, Pluronic P123 (M_n = 5750 g/mol) EO_{20}-$PO_{70}EO_{20}$, where "EO" represents the ethyleneoxide monomer segments and "PO" the propyleneoxide segments of which the poly(ethyleneoxide) (PEO) and poly(propyleneoxide) (PPO) blocks are comprised, was received as a gift from BASF, U.S.A., and used as-received. The conjugated polymers used in this study were purchased from ADS, Canada, and used as received: poly[2-methoxy-5-(2′-ethyl-hexyloxy)-1,4-phenylene vinylene] (MEH-PPV, M_n = 200K), poly(9,9′-dioctylfluorene) (PFO, M_n = 74K), and poly(9,9-dioctylfluorene-*co*-benzothiadiazole) (F8BT, M_n = 40K).

Synthesis of Conjugated Polymer-Incorporated Mesostructured Silica from Aqueous/Ethanolic Sol Solutions. The sol solution was prepared by mixing 1 mL of ethanol with 0.54 mL of 0.01 M HCl and 1.1 mL of tetraethoxysilane for 1 h at 22 °C. For the deposition of the cubic or hexagonal mesostructures, 0.17 or 0.28 g of P123 were dissolved in 1 mL of ethanol, respectively. The surfactant solution was added to the sol solution for additional mixing of about 2 h. The molar ratios in the final sol solutions (prior to addition of the conjugated polymers) were 1: 9:6:x TEOS/ethanol/water/P123 where x = 0.006 or 0.010 for the cubic or hexagonal mesostructures, respectively. Conjugated polymers were then added to the sols by dropwise adding 0.4 mL of xylene solutions of MEH-PPV, PFO, or a blend of both polymers into the sol precursor solutions. The concentration of all the pristine polymer and polymer blend solutions was 2 mg/mL in xylene. A blend of the sol solutions, in contrast to a blend of the polymer solutions, was also prepared, by mixing 2 mL of the MEH-PPV sol solution with 2 mL of the PFO sol solution to obtain 4 mL of the sol solutions mixture. Upon addition of the xylene solution the sol became milky with a slight tint of either red (MEHPPV) or light blue (PFO). The sample for EF-TEM characterization was prepared by dropwise adding 0.4 mL of a 1 mg/mL F8BT in xylene solution to the sol precursor solution.

The conjugated polymer loading, estimated by dissolving freshly prepared films in known amounts of chloroform and determining the concentration of the conjugated polymer in the solution by optical absorption, was found to range between 0.4 and 0.9 wt % of the composite film.

Synthesis of Conjugated Polymer-Incorporated Mesostructured Silica from Aqueous Sol Solutions. The aqueous precursor sol solutions (no ethanol) were prepared by placing 1.50 mL of 0.01 M HCl, 0.50 mL of tetraethoxysilane, and 0.08−0.33 g of P123 (for wormlike to lamellar mesostructure, respectively) for 1 h in an ultrasonic bath, until a clear viscous solution was obtained. Conjugated polymers were then added to the sols by dropwise adding 0.5 mL of xylene solutions of 4 mg/mL MEH-PPV, or PFO, into the aqueous sol precursor solutions. The molar ratios in the final aqueous sol solutions were 1:37:x:4×10^{-6} TEOS/water/P123/conjugated polymer, where x = 0.006 to 0.026 for the wormlike to lamellar mesostructures, respectively.

Synthesis of Conjugated Polymer-Incorporated Mesostructured Titania from Aqueous Sol Solutions. The titania sol solution was prepared by mixing 1.2 mL of hydrochloric acid (HCl, 12 M) with 1.3 mL of titanium tetra-ethoxide under vigorous stirring, until a clear solution was achieved. For the deposition of the cubic or lamellar mesostructures, 0.312 or 0.997 g of P123 were dissolved in the clear sol solution, respectively. The molar ratios in the final sol solutions (prior to addition of conjugated polymers) were 1:2.3:8.1:x TEOT/HCl/water/P123 where x = 0.009 or 0.028 for the cubic or lamellar mesostructures, respectively. Conjugated polymers were then added to the sols by dropwise adding 0.5 mL of 1 mg/mL xylene solutions of PFO and MEH-PPV, separately or consecutively (for polymer blend incorporation). Upon addition of the polymer in xylene solution to the low surfactant concentration sol solution, the sol became milky with a red (MEH-PPV) or blue (PFO) tint; while for high surfactant concentrations the sol solution remained clear even after addition of the polymer in xylene solution.

Thin Film Deposition. Composite films were prepared by substrate dip-coating microscope glass slides or polyimide films into freshly prepared, conjugated polymer included (aqueous or aqueous/ethanolic) sol solutions at a rate of 2 mm/s, 22 °C, and relative humidity of 75%. The films were left to dry in the coating chamber for 24−72 h before characterizing or further treatment.

The conjugated polymer loadings in the mesostructured titania films, estimated from the precoursor solution composition following the method suggested by Alberius et al.,[15] are 0.1 and 0.06 wt % for the rhombohedral and lamellar films, respectively.

Characterization. Glancing incidence small-angle X-ray scattering measurements (GISAXS) were performed on polyimide films using a small-angle diffractometer (Bruker Nanostar, KFF CU 2 K-90) with Cu Kα radiation with λ = 1.542 Å in a "glancing incidence" mode.[36] Transmission electron microscopy (TEM) measurements were performed using a FEI Tecnai T12 G2 transmission electron microscope and Philips CM120 TEM, both operated at 120 keV. The energy filter analysis was conducted on a Titan 80−300 FEG-S/TEM (FEI) equipped with high resolution energy filter, for sub-eV EELS and energy filtered TEM. The samples for TEM characterization were prepared by scraping the films from the polyimide or glass substrates with a sharp knife and placing them directly on a carbon-coated copper grid. A Varian Cary Eclipse spectrofluorometer was used to measure the photoluminescence (PL) spectra, with excitation through vertical cross polarizer to eliminate stray light. The excitation wavelengths used were 490 or 420 nm for MEH-PPV and 380 nm for PFO and samples with both MEH-PPV and PFO.

Device Fabrication. Devices were prepared by spin-coating a 100 nm poly(ethylenedioxythiophene)−poly(styrene sulfonic acid) (PEDOT:PSS) layer on a 12×12 mm^2 ITO substrate, followed by a heat treatment at 110 °C for 2 h under inert conditions. A 200 nm-thick nanocomposite layer was deposited by dip-coating onto the PEDOT:PSS-coated substrate. The device was completed by thermally evaporating eight Ca(50 nm)/Al(150 nm) cathode contacts (pixel size of 1×3 mm^2). LED performances were measured using an Agilent 4155C semiconducting parameter analyzer under inert conditions. Electroluminescence spectra were measured using the Varian Cary Eclipse spectrofluorometer operating in biofluorescence mode (no photoexcitation).

Results and Discussion

The deposition of mesostructured metal oxide films from aqueous/ethanol sols is a result of two concurrent

processes: the self-organization of surfactant species into liquid-crystal-like mesophase domains and the polymerization and cross-linking of the metal-oxide network.[38] These processes are driven by the increasing concentrations of the surfactant and the hydrolyzed metal oxide species, respectively, during solvent evaporation. In this study, a solution of conjugated polymers in xylene was dropwise added to the conventional aqueous/ethanol silica precursor sol solution, in view of incorporating highly hydrophobic species, such as conjugated polymers, into mesostructured metal-oxide matrices during their formation. The molar ratio between the metal oxide precursor, and the block copolymer surfactant, Pluronic P123, in the precursor solution was adjusted according to those known to direct mesophases in the ethanol−water−P123 system (see Experimental Section).[15]

Two conjugated polymers were used: blue emitting polyfluorene (PFO) and a red emitting polyphenylene vinylene derivative (MEH-PPV) as well as a blend of the two. Transparent (>90%) films with a slight yellow or red tint were prepared by dip-coating substrates from P123 sol solutions of PFO or MEH-PPV, respectively. The color confirms the presence of conjugated polymer species in all deposited films, regardless of the type of conjugated polymer used, or the P123/metal molar ratio. The mesostructure obtained in the final composite film is determined by the P123/metal molar ratio and confirmed by transmission electron microscopy (TEM) and glancing-incidence small-angle X-ray scattering (GISAXS).

The TEM image of a film deposited from a PFO-included aqueous/ethanolic sol solution, with P123/Si molar ratio of 0.006:1 (Figure 1a), shows a well resolved 3D cubic ordering with a lattice parameter of ca. 14.0 nm. The bright spheres in the TEM image are associated with the organic domains, while the dark scaffold is the silica matrix. The cubic ordering is corroborated in the 2D GISAXS pattern, Figure 1b, showing sharp, intense (110) and (101) reflections, and a weaker ($1\bar{1}0$) reflection. This pattern is consistent with a highly regular 3D body-centered cubic structure[39] ($Im\bar{3}m$) with a lattice parameter of approximately 14.1 nm, in good agreement with the TEM image (Figure 1a). A schematic illustration of the $Im\bar{3}m$ P123-templated PFO-incorporated silica is also shown in Figure 1b. In contrast, films deposited from PFO-included aqueous/ethanolic precursor solutions with a P123/Si molar ratio of 0.010:1 show a 2D hexagonal mesostructure with arrays of cylinders aligned parallel to the substrate. The 2D GISAXS pattern, Figure 1c, reveals sharp, intense (100) equatorial reflections and weaker ($\bar{1}10$) and (010) reflections. This pattern reflects a highly regular 2D hexagonal structure with a *d*-spacing of 9 nm for the {100} planes, with the cylinders oriented parallel to the substrate. A schematic illustration of the 2D hexagonal P123-templated PFO-incorporated silica is also shown in Figure 1c. Dip-coating substrates into

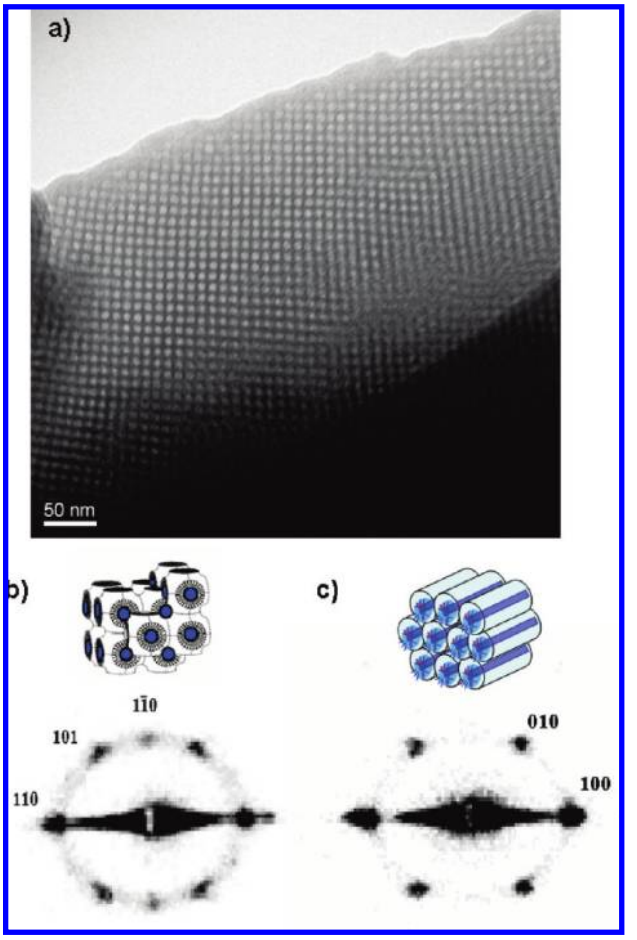

Figure 1. (a) TEM image of a well-ordered PFO-incorporated P123-templated cubic composite film deposited from an aqueous/ethanolic precursor sol solution with P123/Si molar ratio of 0.006:1, viewed along the (100) plane, and 2D GISAXS patterns and schematic illustrations of PFO-incorporated P123-templated silica films: (b) 3D-cubic, (same as a) and (c) PFO-incorporated P123-templated 2D-hexagonal composite film deposited from an aqueous/ethanolic precursor sol solution with a P123/Si molar ratio of 0.010:1. The blue spheres and cylinders in the schemes represent PFO conjugated polymer species positioned in the surfactant P123 micelles, enclosed within the silica matrix.

MEH-PPV-included aqueous/ethanolic precursor sol solutions with the P123/Si molar ratios of 0.006:1 or 0.010:1 leads to the deposition of MEH-PPV-incorporated 3D-cubic or 2D-hexagonal silica films, respectively, indicating that the type of conjugated polymer used in the synthesis does not affect the obtained mesostructure.

Direct and unambiguous determination of the conjugated polymer location in the mesostructured films was obtained, for the first time, using energy filtered TEM (EF-TEM). The sub-eV energy-filtered resolution provides the ability to map the distribution of a single element, sulfur in this case, on a high resolution image. Here, films deposited from an aqueous/ethanolic precursor solution with a sulfur-baring conjugated polymer, F8BT, were used to establish the location of the polymer guest species in the mesostructured hybrid film. The bright field TEM image of an F8BT-incrporated P123-directed silica film, Figure 2a, shows hexagonally packed organic cylinder arrays (bright signals) viewed from the (001) plane with a periodic spacing of approximately

(38) Soler-Illia, G. J. A. A. *Chem.—Eur. J.* **2006**, *12*(17), 4478–4494.
(39) Grosso, D.; Soler-Illia, G.; Crepaldi, E. L.; Cagnol, F.; Sinturel, C.; Bourgeois, A.; Brunet-Bruneau, A.; Amenitsch, H.; Albouy, P. A.; Sanchez, C. *Chem. Mater.* **2003**, *15*(24), 4562–4570.

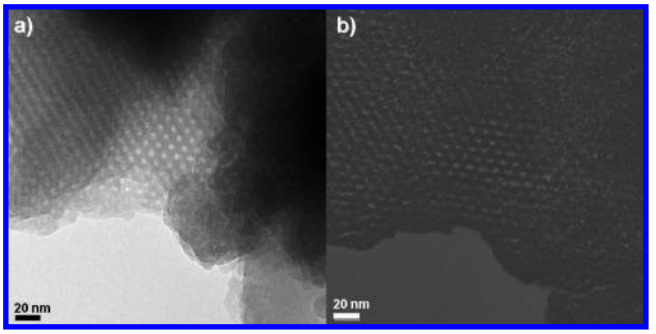

Figure 2. (a) TEM image of a well-ordered F8BT-incorporated P123-templated hexagonal mesostructured nanocomposite film deposited from a precursor solution with a P123/Si molar ratio of 0.010:1, viewed along the (001) plane; (b) an energy-filtered TEM image of the same region shown in (a). The bright spots in (b) correspond to the presence of sulfur in the film, that is, the location of the F8BT conjugated polymer.

9 nm, in agreement with the PFO-incorporated P123-directed silica film (Figure 1c). Figure 2b shows a TEM image of the same area shown in Figure 2a; however, in this case the image is constructed only by electrons that have interacted with sulfur atoms in the film. The energy-filtered TEM image (Figure 2b) is achieved by applying the energy filter to select only electrons with energy loss associated to the L23-edge of sulfur atoms at 165 eV. Therefore, the bright spots in Figure 2b represent regions where electrons passing through the film interacted with sulfur atoms, while the dark regions indicate no electron−sulfur interactions. Comparing the two images in Figure 2 shows that the sulfur distribution completely follows the shape and spatial arrangement of the surfactant channels. This direct evidence proves unambiguously that the conjugated polymer is not macrophase separated but, rather, incorporated and well distributed in the organic channels of the mesoperiodic silica.

Positioning the conjugated polymers in the organic channels of mesostructured silica films, as evident from the TEM, is a result of conjugated polymer-in-xylene addition to the aqueous/ethanol precursor sol solution. During ethanol evaporation the water/xylene incompatibility directs the xylene and conjugated polymers into the hydrophobic domains of the concurrently self-organizing surfactant micelles. Further solvent evaporation induces formation of liquid crystalline-like surfactant assemblies, fixed by the cross-linking of the silica framework. Consequently, the conjugated polymer guest molecules are positioned in the organic domains of the mesostructured silica, as evident from the EF-TEM. However, the partial solubility of xylene in ethanol limits the amount of hydrophobic polymer that can be introduced to the polar solution without polymer sedimentation. Therefore, increasing the polymer uptake into the mesostructure can be done by using an aqueous precursor solution with no ethanol. In the absence of ethanol, addition of xylene to an aqueous sol containing the metal oxide precursor, HCl, and surfactant leads to the immediate formation of an emulsion, similar to that reported by Kiezke et al.[40]

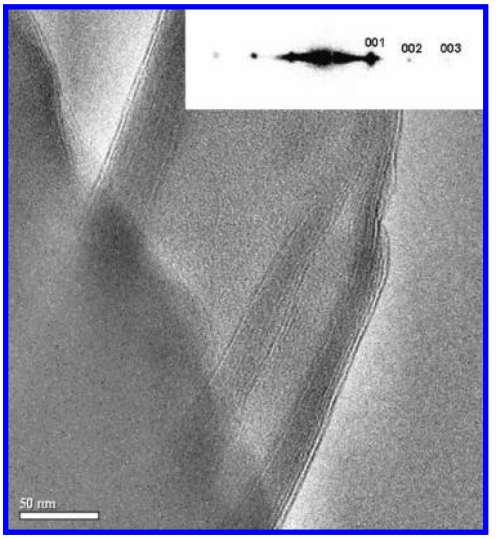

Figure 3. TEM image and a GISAXS pattern (inset) of P123-templated lamellar silica films deposited from aqueous precursor solutions, with no ethanol and a P123/Si ration of 0.026:1. The TEM image is of a film prepared with no conjugated polymer, while the GISAXS pattern, d = 11.5 nm, is of a film prepared from a similar sol solution with PFO.

Films deposited from the emulsions (aqueous/xylene sols), with surfactant concentrations known to direct mesostructured silica from aqueous/ethanolic sols, attain high mesostructure ordering ranging from nonoriented wormlike (low surfactant concentration) to well-ordered lamellar mesostructures (high surfactant concentration). A typical lamellar silica film, deposited from an emulsion prepared by dropwise adding xylene to a P123-included aqueous precursor solution (no ethanol), is shown in the TEM image of Figure 3. The image shows a stripe pattern with variable spacing distances between the stripes, a result of a diagonal cut through the stack of lamella. The GISAXS pattern, shown in the inset of Figure 3, shows three well resolved sharp diffraction points directed out of plane, confirming the formation of a well ordered lamellar structure with d-spacing of 11.5 nm.

The synthesis of conjugated polymer-incorporated mesostructured silica from aqueous sol solutions was performed by dropwise adding conjugated polymers in xylene solutions to aqueous precursor sol solutions containing a metal oxide precursor, HCl, and surfactant, with no alcoholic solvent.[41] Emulsions are formed in the aqueous sols with a blue or red tint, depending on the conjugated polymer species, PFO or MEH-PPV, respectively. Films deposited from the conjugated polymer-incorporated emulsions show the same mesostructures observed for films deposited from the same emulsion composition (Figure 3), but with no conjugated polymer, and maintain the color of the emulsion, red for MEHPPV and blue for PFO. No apparent macrophase separated conjugated polymer domains are observed in the films, supporting the distribution of the conjugated polymer chains in the organic domains of the composite films.

(40) Kietzke, T.; Neher, D.; Landfester, K.; Montenegro, R.; Guntner, R.; Scherf, U. *Nat. Mater.* **2003**, *2*(6), 408–412.

(41) Martini, I. B.; Craig, I. M.; Molenkamp, W. C.; Miyata, H.; Tolbert, S. H.; Schwartz, B. J. *Nat. Nanotechnol.* **2007**, *2*(10), 647–652.

Under the conditions of the aqueous sol, the conjugated polymers are encapsulated by the surfactant in the xylene droplets of the emulsion. Solvent evaporation induces surfactant mesophase formation and silica condensation which fixes the conjugated polymer-incorporated surfactant assembles in a silica scaffold. These aqueous conditions resemble the conditions generated in the aqueous/ethanolic precursor sol solution after ethanol evaporation, that is, during the final stages of the film forming process. Hence, the addition of conjugated polymers in a cosolvent to aqueous or aqueous/ethanolic precursor solutions leads to the deposition of highly ordered, mesostructured silica films, with the conjugated polymer guest molecules positioned in the organic domains of the mesostructure. However, the removal of the mediating solvent, ethanol, results in the formation of a viscous gel with low film-forming properties, leading to the formation of gel-like films with limited feasibility for integration into electronic or optoelectronic applications.

The synthetic approach presented here is general and could be extended for the preparation of functional conjugated polymer-incorporated mesostructured metal oxide films. A desired application is photovoltaic devices based on PPV-type conjugated polymers incorporated into a titanium dioxide host.[42] Therefore, we demonstrate the generality of the cosolvent approach by deposition of conjugated polymer-incorporated mesostructured titania films. First, aqueous titania precursor solutions including a titania precursor, HCl, and surfactant, with no ethanol, were prepared. Dip-coating resulted in the deposition of highly ordered mesostructured titania films, with phase-type depending on surfactant concentration. The GISAXS pattern of a film deposited from an aqueous titania precursor solution with low surfactant concentration, P123/Ti molar ratio of 0.009:1 (see Experimental Section), shows a distorted cubic $Im\bar{3}m$ mesostructure (Figure 4a).[13] The *d*-spacing calculated from the diffraction pattern, 9 nm, is similar to that obtained by Alberius et al. for the same volume fraction of P123 in a aqueous/ethanolic conventional titania precursor solution[15] and corresponds to an average lattice parameter of 13 nm. Increasing surfactant concentration to a P123/Ti molar ratio of 0.028:1 results in the formation of a lamellar mesostructure, as shown in the GISAXS pattern in Figure 4b. The lattice spacing of the lamellar mesostructure, 11 nm, is comparable with that obtained by Alberius et al.[15] for lamellar titania films template by P123.

When conjugated polymer in xylene solutions were dropwise added to the aqueous titania precursor solutions, the solution with low surfactant concentration (P123/Ti molar ratio of 0.009:1) appeared milky, while that with high surfactant concentration (P123/Ti molar ratio of 0.028:1) remained clear. This noticeable difference indicates the presence of relatively large emulsion droplets in the low surfactant concentration solution, while the high surfactant concentration stabilizes an emulsion with smaller droplets (high surface area). Dip coating from both solutions leads to the deposition of highly ordered conjugated-polymer-incorporated mesostructured titania films. Figure 4c shows the GISAXS pattern of a film deposited by adding MEH-PPV in xylene to the aqueous titania precursor solution with low surfactant concentration. The pattern includes 10 well resolved diffraction spots (Figure 4c), reflecting a combination of rhombohedral and hexagonal mesostructures. The rhombohedral structure, with a d_{111}-spacing of about 11 nm corresponding to a lattice parameter of ~15 nm, is a result of an uneven contraction of a cubic mesostructure, as previously reported for conventionally prepared cubic silica and titania templated by P123.[43,44] The slight increase in the lattice parameter upon addition of conjugated polymers and xylene to the precursor solution, from 13 to 15 nm, could be indicative of surfactant domain swelling by xylene incorporation into the hydrophobic cores of the P123 micelles. This increase of hydrophobic domain-size in the surfactant assemblies also reduces the assembly curvature inducing the appearance of the hexagonal mesostructure. The presence of the

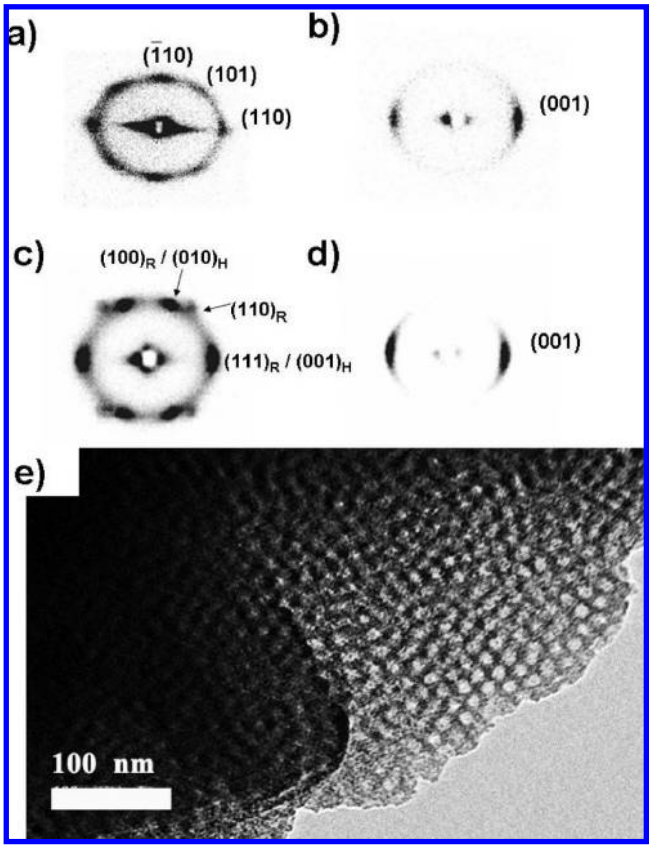

Figure 4. GISAXS patterns of P123-templated titania films prepared from aqueous titania precursor solutions: (a, b) without addition of MEH-PPV in xylene and (c, d) with the addition of MEH-PPV in xylene. The P123/Ti molar ratios in the precursor solution were (a, c) 0.009:1 and (b, d) 0.028:1. (e) TEM image of a sample corresponding to the GISAXS pattern in (c).

(42) Ravirajan, P.; Haque, S. A.; Durrant, J. R.; Bradley, D. D. C.; Nelson, J. *Adv. Funct. Mater.* **2005**, *15*(4), 609–618.

(43) Choi, S. Y.; Lee, B.; Carew, D. B.; Mamak, M.; Peiris, F. C.; Speakman, S.; Chopra, N.; Ozin, G. A. *Adv. Funct. Mater.* **2006**, *16* (13), 1731–1738.

(44) Eggiman, B. W.; Tate, M. P.; Hillhouse, H. W. *Chem. Mater.* **2006**, *18*(3), 723–730.

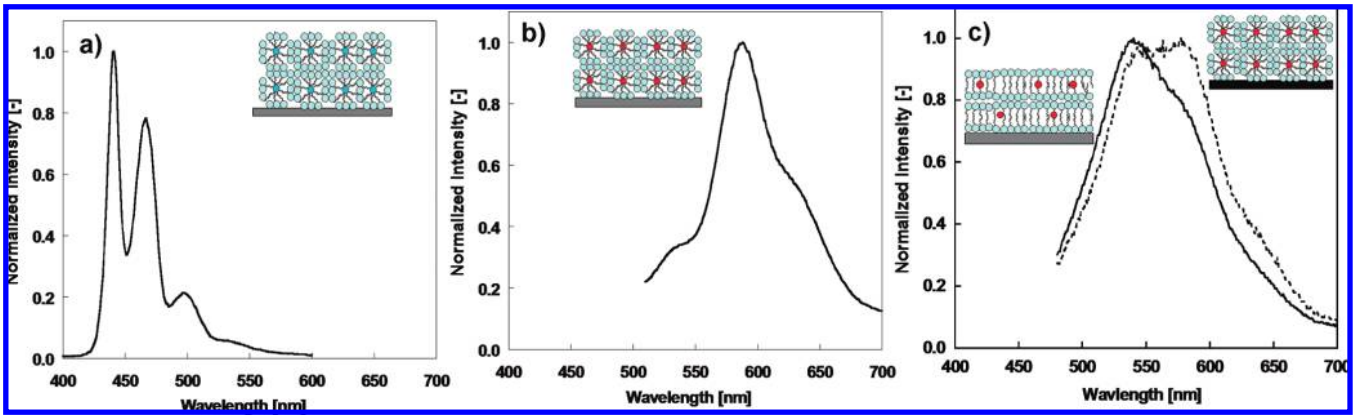

Figure 5. Photoluminescence spectra and schematic illustrations of (a) a PFO-incorporated cubic silica film excited at 380 nm; (b) a MEH-PPV-incorporated cubic silica film excited at 490 nm; and (c) MEH-PPV-incorporated titania rhombohedral (dashed line) and lamellar (solid line) films excited at 420 nm.

hexagonal mesostructure is corroborated by TEM, Figure 4e, showing the 6-fold typical hexagonal symmetry. The center-to-center distance between the organic domains (bright regions) in the TEM image is 14 nm, in agreement with the corresponding GISAXS hexagonal pattern in Figure 4c. The GISAXS pattern of MEH-PPV-incorporated films deposited from aqueous titania precursor solutions with high P123 concentrations shows well resolved out-of-plane diffraction spots identified as the (001) plane of the lamellar mesophase (Figure 4d). The lamellar lattice spacing, 11−11.5 nm, is slightly higher than that obtained for films deposited from aqueous titania precursor solutions, indicating swelling of the surfactant assemblies by xylene. Notably, the quality of the mesostructured titania films deposited using this emulsion process is low due to the formation of gel-like films with limited possibility for integration into electronic or optoelectronic applications.

The optical properties and photophysical processes in conjugated polymers are extremely sensitive to their local environment and hence can be used here to corroborate conjugated polymer encapsulation in the organic domains of the mesostrucuterd films.[45] In general, photoluminescence (PL) spectra of the conjugated polymer-incorporated mesostructured metal oxide films prepared in this study indicate that the conjugated polymers maintain their optical properties upon incorporation into the films. For example, the PL spectrum of a PFO-incorporated cubic silica film, Figure 5a, is typical of PFO films showing the 0−0, 0−1, and 0−2 vibronic transitions at 440, 466, and 498 nm, respectively.[46] A similar PL spectrum was obtained from the PFO-incorporated hexagonal silica film (not shown). The PL features of PFO incorporated into titania (not shown) are similar to those of PFO incorporated into silica (Figure 5a), indicating that the PFO maintains its optical properties also in the titania matrix.

The PL spectrum of a MEH-PPV-incorporated cubic silica film shows an emission peak centered at 587 nm and a shoulder at 635 nm (Figure 5b), both features typical of pristine MEH-PPV films, associated with the 0−0 and 0−1 transitions, respectively.[47] However, the PL of the incorporated MEH-PPV also shows an emission peak at 540 nm, which is not observed in pristine polymer films (Figure S1 in Supporting Information). The appearance of the high energy emission peak could be associated with the presences of short conjugated polymer chains and suppressed energy transfer from the high energy segments (short conjugation) to low energy (long conjugated) segments.[22,48] Short conjugation segments may result either from changes in conformation when incorporated into the matrix or physical defects induced by residual water or ethanol molecules present in the film during the drying process.[49,50] Furthermore, selective positioning of the conjugated polymers in the hydrophobic surfactant cores suppresses energy transfer between surfactant domains separated by the surfactant hydrophilic corona and silica scaffold walls. Nanoencapsulation of chromophores to control energy transfer has been demonstrated by dye incorporation into zeolites,[51] layered compounds,[52] dendrimers,[53] and cyclodextrins[54] which were used to enhance electroluminescence in a LED and, very recently, in diblock copolymer micelles.[55]

Suppression of energy transfer between conjugated polymers incorporated into a metal oxide scaffold is also observed in the PL spectra of MEH-PPV-incorporated titania films, Figure 5c, which show broader and

(45) Schwartz, B. J. *Annu. Rev. Phys. Chem.* **2003**, *54*(1), 141–172.
(46) Scherf, U.; List, E. J. W. *Adv. Mater.* **2002**, *14*(7), 477–487.
(47) Nguyen, T. Q.; Martini, I. B.; Liu, J.; Schwartz, B. J. *J. Phys. Chem. B* **2000**, *104*(2), 237–255.
(48) Wu, J. J.; Gross, A. F.; Tolbert, S. H. *J. Phys. Chem. B* **1999**, *103* (13), 2374–2384.
(49) Padmanaban, G.; Ramakrishnan, S. *J. Phys. Chem. B* **2004**, *108* (39), 14933–14941.
(50) Traiphol, R.; Sanguansat, P.; Srikhirin, T.; Kerdcharoen, T.; Osotchan, T. *Macromolecules* **2006**, *39*(3), 1165–1172.
(51) Wada, Y.; Sato, M.; Tsukahara, Y. *Angew. Chem., Int. Ed.* **2006**, *45* (12), 1925–1928.
(52) Aharon, E.; Kalina, M.; Frey, G. L. *J. Am. Chem. Soc.* **2006**, *128* (50), 15968–15969.
(53) Kim, G. W.; Cho, M. J.; Yu, Y. J.; Kim, Z. H.; Jin, J. I.; Kim, D. Y.; Choi, D. H. *Chem. Mater.* **2007**, *19*(1), 42–50.
(54) Brovelli, S.; Latini, G.; Frampton, M. J.; Mcdonnell, S. O.; Oddy, F. E.; Fenwick, O.; Anderson, H. L.; Cacialli, F. *Nano Lett.* **2008**, *8* (12), 4546–4551.
(55) Yoo, S. I.; J. A., S.; Choi, G. H; Kim, K. S.; Yi, G. C.; Zin, W. C.; Jung, J. C; Sohn, B. H. *Adv. Mater.* **2007**, *19*(12), 1594–1596.

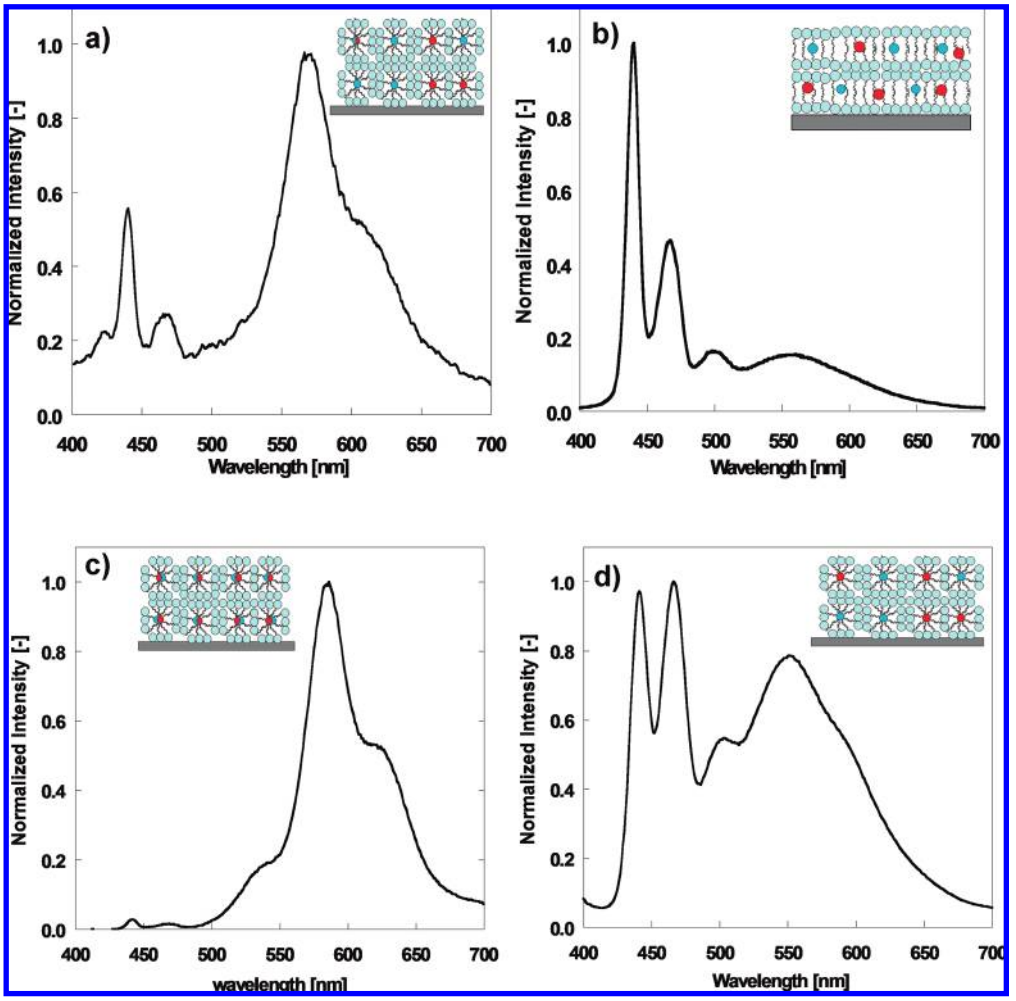

Figure 6. Photoluminescence spectra and schematic illustrations of MEH-PPV- and PFO-incorporated mesostructured metal oxide films: (a) rhombohedral titania with MEH-PPV and PFO separately introduced into the precursor solution; (b) lamellar titania with MEH-PPV and PFO separately introduced into the precursor solution; (c) a polymer blend-incorporated cubic silica film; (d) a cubic silica film prepared from a mixture of PFO-included and MEH-PPV-included precursor solutions. All films were excited at 380 nm.

blue-shifted features compared with pristine MEH-PPV films. The PL spectrum of a rhombohedral MEH-PPV-incorporated titania film (dashed line in Figure 5c) shows two broad peaks centered at 540 and 580 nm, with almost equal intensities. The appearance of the high energy peak (540 nm) is attributed to both the presence of short conjugated polymer segments and only partial energy transfer between polymer chains (as mentioned above). This assignment is also supported by steady-state polarized photoluminescence measurements (Figure S2 in Supporting Information).

In the PL spectrum of a lamellar MEH-PPV-incorporated titania film (solid line in Figure 5c), the 540 nm peak becomes significantly stronger than the 580 nm peak indicating that energy transfer suppression is more pronounced in the lamellar phase compared to the romboherdal phase. Although the lamellar phase is more interconnected than the rhombohedral phase, MEH-PPV chains are more effectively isolated by surfactant molecules in the lamellar phase because the surfactant/MEH-PPV ratio is three times higher than that in the rombohedral phase. Accordingly, conjugated polymer chains incorporated into the lamellar phase are more likely to be encapsulated by surfactant molecules leading to higher separation between the chromophores of the conjugated polymers and efficient suppression of energy transfer.

Further evidence supporting the suppression of energy transfer between polymer chains incorporated into the titania films is obtained by incorporating both the blue- and the red-emitting polymers into one titania film. Proximity between these polymers causes efficient energy transfer from the blue to the red emitting polymer, resulting solely in red emission (Supporting Information, S3). In this case, the two polymers were *separately* introduced into the aqueous titania precoursor solution by first dropwise adding PFO in xylene to the precursor solution followed by dropwise adding MEH-PPV in xylene to the same solution. Figure 6a,b shows the PL spectra of rhombohedral and lamellar titania films, respectively, both deposited from precursor solution containing both MEH-PPV and PFO. The excitation wavelength was 380 nm which excites preferentially the PFO polymer. Despite the preferential PFO excitation, the PL spectrum of the rhombohedral titania shows emission form both the red- and the blue-emitting polymers (Figure 6a), evident of partial energy transfer between the excited

PFO to near MEH-PPV chains in the rhombohedral phase. Furthermore, the PL spectrum of the lamellar titania shows emission from the blue-emitting polymer only (Figure 6b), confirming the suppression of energy transfer between spatially separated PFO and MEH-PPV incorporated in the lamellar phase. Suppression of energy transfer is more efficient in the lamellar phase compared to the rhombohedral phase due to the higher concentration of surfactant in the lamellar phase which isolates polymer chains more efficiently. Notably, surfactant molecules act as spacer not only between conjugated polymer chains but also between the incorporated conjugated polymers, suppressing also MEH-PPV PL quenching by the titania matrix.

The suppression of energy transfer between conjugated polymer chains incorporated into the organic domains of metal oxide mesostructured films is also demonstrated by incorporating both MEH-PPV and PFO into cubic silica films deposited from aqueous/ethanolic solutions. The red- and blue-emitting conjugated polymers were dropwise introduced into the precursor solution either jointly or separately. In the former, the two polymers were first blended together in xylene and then collectively dropwise added to the aqueous/ethanolic surfactant-included precursor solution. Under these conditions, the surfactant micelles formed in the solution are likely to contain *both* red- and blue-emitting conjugated polymer chains. In the second case, each conjugated polymer was dropwise added from xylene into an aqueous/ethanolic surfactant-included precursor solution, and then the two precursor solutions were mixed keeping each polymer-type isolated in different micelles. Under these conditions each micelle is likely to contain either red- or blue-emitting conjugated polymer chains.

The PL spectrum of a cubic silica composite film deposited from the precursor solution of the polymer blend, Figure 6c, exhibits intense emission from the red-emitting polymer and only very weak signals from the blue-emitting polymer. In contrast, the PL spectrum of the cubic silica composite film deposited from the solution with monochromatic blue-emitting or red-emitting micelles, Figure 6d, exhibits white emission, that is, intense emission from both the red- and the blue-emitting polymers, simultaneously. The dramatic difference between the PL spectra of the two films is due to the different dynamics of energy transfer from the high band gap blue-emitting PFO to the low band gap red-emitting MEH-PPV in both cases. When the two polymers are collectively incorporated in a micelle, photoexcitation of the PFO is efficiently and rapidly transferred to MEH-PPV, resulting in nearly pure red-emission, as shown in Figure 6c. However, when the PFO and MEH-PPV are positioned in different micelles, the spatial separation between the micelles suppresses energy transfer from the blue-emitting PFO to the red-emitting MEH-PPV, leading to blue- and red-emission in concert, that is, white emission.[52,56]

The combination of red and blue emission contributions in Figure 6d indicates partial energy transfer from PFO to MEH-PPV despite the ~5 nm spatially separating between two adjacent micelles, a distance larger than the expected Förster radius, about 4 nm.[57,58] This partial energy transfer could be associated with partial intermixing between the micelles that contain PFO and MEH-PPV polymers during film processing and/or with interconnection between neighboring micelles which allows micelle-to-micelle connectivity in the cubic mesostructures. Therefore, positioning the conjugated polymers in the micelles not only offers control over energy transfer between micelles leading to white emission but also may provide conductive pathways for charge transfer through the composite film. The propagation of charge carriers along and between conjugated polymer chains is the fundamental physical process in polymer electronics.[59−61] Indeed, 3D cubic conjugated polymer-incorporated titania and silica films were recently advantaged for photovoltaic devices (PVs),[37] and light-emitting diodes (LEDs),[14] respectively. Accordingly, integration of the conjugated polymer-incorporated 3D-cubic silica films prepared in this study as the active layer in LED structures resulted in diode-like behavior and light generation, while the conjugated polymer-incorporated 2D-hexagonal silica films showed no rectification or light output (see Supporting Information, S4).

The efficacy of the white-emitting cubic silica composite film prepared from the mixture of MEH-PPV and PFO precursor solutions for white electroluminescent devices is tested by integrating the composite film as the active layer in an LED. The device configuration was ITO/ poly(ethylenedioxythiophene):poly(styrene sulfonic acid) ~80 nm/composite film ~200 nm/Ca 50 nm/Ag 150 nm. The current density−field−luminance curves (JVL) and EL spectrum of the 3D cubic composite device are shown in Figure 7. The EL spectrum (Figure 7 inset) shows noticeable blue and red contributions yielding white CIE coordinates (0.27, 0.36, see Supporting Information Figure S6), similar to the PL spectrum of the same film (Figure 6d), although the vibronic transitions of both polymers are not resolved. Furthermore, the EL spectrum also shows a significant contribution in the green region, 500−550 nm, generated by green-emitting defects in PFO and MEH-PPV with short conjugated segments.[46,50] The PFO green emission, attributed to the formation of keto-defects[62] and/or intermolecular species,[63] was also

(56) Yoo, S. I.; Lee, J.-H.; Sohn, B.-H.; Eom, I.; Joo, T.; Jin An, S.; Yi, G.-C. *Adv. Funct. Mater.* **2008**, *18*(19), 2984–2989.
(57) Chen, H. C.; Wang, C. T.; Liu, C. L.; Liu, Y. C.; Chen, W. C. *J. Polym. Sci., Part B: Polym. Phys.* **2009**, *47*(5), 463–470.
(58) Meskers, S. C. J.; Hubner, J.; Oestreich, M.; Bassler, H. *J. Phys. Chem. B* **2001**, *105*(38), 9139–9149.
(59) Friend, R. H.; Gymer, R. W.; Holmes, A. B.; Burroughes, J. H.; Marks, R. N.; Taliani, C.; Bradley, D. D. C.; Dos Santos, D. A.; Bredas, J. L.; Logdlund, M.; Salaneck, W. R. *Nature* **1999**, *397* (6715), 121–128.
(60) Scott, J. C.; Bozano, L. D. *Adv. Mater.* **2007**, *19*(11), 1452–1463.
(61) Gunes, S.; Neugebauer, H.; Sariciftci, N. S. *Chem. Rev.* **2007**, *107* (4), 1324–1338.
(62) Romaner, L.; Pogantsch, A.; de Freitas, P. S.; Scherf, U.; Gaal, M.; Zojer, E.; List, E. J. W. *Adv. Funct. Mater.* **2003**, *13*(8), 597–601.
(63) Chen, X. W.; Tseng, H. E.; Liao, J. L.; Chen, S. A. *J. Phys. Chem. B* **2005**, *109*(37), 17496–17502.

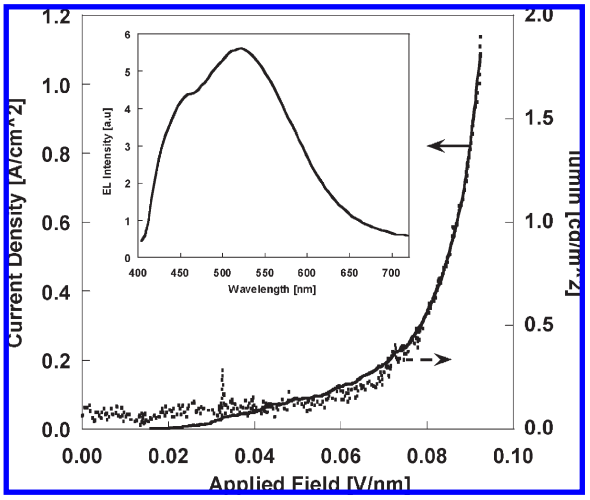

Figure 7. JVL characteristics and EL spectrum (inset) of light emitting diodes based on a PFO- and MEH-PPV-included 3D-cubic 200 nm thick, silica film.

observed in the EL spectrum of 3D cubic PFO-incorporated silica films (see Supporting Information, Figures S5 and S6) and has been previously utilized for green emission in white PLEDs.[64] Oxidation of the polyfluorene from the keto-defect occurs despite the encapsulation of the polymer in the surfactant domains probably due to the presence of water in the solution and to the ambient conditions in which the devices are prepared. The relatively high turn-on voltage and low brightness of the white EL device, ~2 cd/m^2 at 20 V, are probably due to the insulating character of the silica host matrix which inhibits charge transfer and the low polymer uptake in the composite film limited by the stability of the conjugated polymer in the sol solution, respectively.

Summary and Conclusions

This study reports the incorporation of conjugated polymers into the organic domains of block copolymer templated mesostructured metal oxides. This method has permitted the deposition of conjugated polymer-incorporated 2D-hexagonal and 3D-cubic silica and titania films from predominantly aqueous conditions. The conjugated polymers were first dissolved in xylene and then dropwise added into aqueous or aqueous/ethanolic solutions including a block copolymer surfactant and a metal oxide precursor species. Depending on surfactant concentration and type of metal-oxide precursor, conjugated polymer-incorporated 2D-hexagonal and 3D-cubic silica and titania films could be achieved. The hydrophobic and less volatile cosolvent, xylene, swells the block copolymer surfactant micelle cores and drives the conjugated polymer guests into the organic domains of the self-assembling liquid crystalline-like mesophases that template the metal oxide scaffold. Confining the guests to the organic domains of the mesostrutured films suppresses energy transfer between conjugated polymers located in adjacent domains separated by the metal oxide scaffold walls. Accordingly, separate inclusion of red- and blue-emitting polymers in mesostructured silica and titania films resulted in simultaneous blue and red emission, that is, white light generation. Furthermore, the white-emitting 3D-cubic silica film, which supports carrier transport along the continuous through-film conjugated polymer pathways, was integrated as the active layer in white light emitting devices. The methodology presented here for the generation of white emission by encapsulation of conjugated polymers in block copolymer micelles can be easily and simply extended to achieve the desired target of secondary and ternary color electroluminescence by judicious mixing of RGB "monochromatic" metal oxide precursor solutions.

Acknowledgment. We wish to thank Dr. Yaron Kauffman of the Materials Engineering Electron Microscopy Centre for performing the EF-TEM measurements.

Supporting Information Available: PL spectra of a pristine MEH-PPV film; polarized PL spectra of rhombohedral titania/P123/MEH-PPV; PL spectra of a film deposited from a blend of MEH-PPV and PFO; JVL characteristics and luminescence spectra of PFO-incorporated mesostructured silica; photoluminescence and electroluminescence spectra of the 3D cubic PFO-incorporated silica; and CIE coordinates corresponding to LED devices prepared in this study (PDF). This material is available free of charge via the Internet at http://pubs.acs.org.

(64) Sun, Q. J.; Fan, B. H.; Tan, Z. A.; Yang, C. H.; Li, Y. F.; Yang, Y. *Appl. Phys. Lett.* **2006**, *88*(16), 163510.